



Improved ionic conductivity and efficiency of dye-sensitized solar cells with the incorporation of 1-methyl-3-propylimidazolium iodide

Chee Yu Tan¹ · Norshahirah M. Saidi¹ · N.K. Farhana¹ · Fatin Saiha Omar¹ · Mohammed M. Algaradah² · Shahid Bashir¹ · S. Ramesh¹ · K. Ramesh¹

Received: 14 September 2019 / Revised: 5 December 2019 / Accepted: 5 January 2020 / Published online: 17 January 2020
© Springer-Verlag GmbH Germany, part of Springer Nature 2020

Abstract

1-Methyl-3-propylimidazolium iodide (MPII) ionic liquid incorporated gel polymer electrolyte (GPE) has successfully enhanced the efficiency of a dye-sensitized solar cell (DSSC). A series of gel polymer electrolytes containing different amounts of MPII were prepared and characterized. A maximum ionic conductivity of 3.99 mS cm^{-1} was obtained in a GPE containing 10 wt% MPII, which was accompanied by the lowest activation energy. The results from dielectric studies showed typical behaviour for both ϵ' and ϵ'' in which their values decreased with increasing frequency but increased proportionately with temperature. From the results of FESEM, the morphologies of the GPE became slightly rougher after the addition of MPII. Dye-sensitized solar cells were fabricated and characterized using electrochemical impedance spectroscopy (EIS) and photovoltaic studies. DSSC with the best performance (4.35% of efficiency, 9.97 mA cm^{-2} of J_{SC} , 0.67 V of V_{OC} , and 65.39% of fill factor) was assembled using the GPE with 10 wt% of MPII.

Keywords Dye-sensitized solar cell · Gel polymer electrolyte · Ionic liquid · Dielectric studies · Fourier-transform infrared spectroscopy

Introduction

DSSC has been one of the most promising candidates for harvesting the solar energy since it has been reported by Brian O' Regan and Michael Grätzel [1]. Typical DSSC consists of several main components which include a working electrode made of both titanium dioxide (TiO_2) nanoparticles and dye molecules, a liquid electrolyte and a platinum-covered-counter electrode [1]. Although liquid-based DSSCs have shown to have efficiency as high as 14% (with collaborative sensitization by silyl-anchor and carboxy-anchor dyes), the usage of liquid electrolyte also carries a number of disadvantages [2]. Liquid electrolytes are generally based on organic solvents that are highly volatile and at risk of evaporating

over time within devices. In this case, the performance of liquid electrolyte based DSSCs diminishes, making this class of devices less viable for long-term applications. In addition, the presence of liquid component also requires costly manufacturing processes to seal the DSSC perfectly in order to prevent leakage.

One of the alternatives for the liquid electrolytes are gel polymer electrolytes (GPEs). Advantages of using GPEs in DSSCs include low probability of leakage problem and high thermal and chemical stability. GPEs consist of polymer matrix, iodide salt, iodine, and solvent. Despite their relatively high thermal and long-term stability, the incorporation of polymer chains to form electrolyte gels can often hinder the mobility of ionic charge carriers, leading to an overall decrease in ionic conductivity. This issue has been partly overcome in GPEs by employing polymers with a low degree of crystallinity in which the ionic conductivity of charge carriers benefits from less ordered amorphous regions within the electrolyte matrix [3].

Recently, copolymers have attracted enormous attention to be used as the host polymers in electrolytes. Poly (vinyl alcohol-co-ethylene) (PVA-co-PE) copolymer able to adopt a highly amorphous quasi-solid-state and present a large

✉ S. Ramesh
rameshtsubra@gmail.com

¹ Centre for Ionics University of Malaya, Department of Physics, Faculty of Science, University of Malaya, 50603 Kuala Lumpur, Malaysia

² King Khalid Military Academy, Riyadh 11495, Saudi Arabia

number of polar groups on the PVA component that can interact with ionic redox couples within the GPE matrix. Although both polyvinyl alcohol and polyethylene are highly crystalline polymers, the copolymerization process greatly reduces the crystallinity of PVA-*co*-PE by interrupting the orderly arrangement of the two polymers [4]. Polar groups present in PVA-*co*-PE may potentially increase the ionic conductivity by facilitating the transport of ions. However, the incorporation of polymer into the electrolyte would reduce the density of free charge carriers since polymer itself does not dissociate into free ions. Therefore, ionic liquids (ILs) are being added into the GPEs as additives. ILs are salts that consist of cations and anions in molten state at ambient temperature [5]. ILs stay in liquid form over a large range of temperatures, attributed to the fact that they have high boiling points and a low melting point at the same time. Moreover, they are non-volatile and have been shown to exhibit high ionic conductivity (approximately 10^{-3} mS cm^{-1}). Different types of imidazolium iodide-based ionic liquids such as 1-methyl-3-propylimidazolium iodide (MPII), 1-butyl-3-methylimidazolium (BMII), and 1-hexyl-3-methylimidazolium iodide (HMII) are suitable to be used as the additive for the improvement of GPE's ionic conductivity, contributed from the presence of non-volatile imidazolium ring in their chemical structure. In this study, MPII has been chosen as the additive to PVA-*co*-PE-based GPEs as it has the shortest alkyl group of imidazolium iodide with relatively poor van der Waals forces that can prevent the cation aggregation. Besides, MPII ionic liquid has low viscosity which able to enhance the transportation of charge carrier within the electrolyte and further enhance their photovoltaic performance of DSSC [6–8].

In this paper, the IL-based GPEs were prepared using MPII and PVA-*co*-PE to fabricate highly efficient DSSCs. The ionic conductivity and dielectric behaviour of the prepared GPE were studied. The complexation between the ionic liquid and copolymer was investigated using Fourier-transform infrared (FTIR) spectroscopy. The degree of the crystallinity of the GPEs was reported based on the results of X-ray diffraction (XRD) techniques. The application of the GPEs in DSSCs is also reported.

Experimental section

Preparation of MPII-GPEs

The co-polymer, PVA-*co*-PE (68 mol% of vinyl alcohol), dimethyl sulfoxide (DMSO), ruthenium dye (N719), 1-methyl-3-propylimidazolium iodide (MPII) ionic liquid, and sodium iodide (NaI) salt were obtained and used without further treatment from Sigma-Aldrich (Kuala Lumpur, Malaysia). Iodine (I_2) was acquired from Friendemann Schmidt Chemical

(Kuala Lumpur, Malaysia). GPEs were prepared by employing a formulation that was previously optimized according to the procedures reported in the literature [9]. NaI (0.80 g) salt was dissolved in DMSO (5 mL) at room temperature before adding I_2 (135 mg), and the desired quantity of MPII ionic liquid. Table 1 summarizes the composition of MPII-modified GPEs investigated in this work. The maximum concentration of MPII was limited to 15 wt% in order to ensure that gelation at room temperature would occur. While stirring, PVA-*co*-PE was added into the mixture and stirred at 110 °C for 3 h in order to achieve complete dissolution. The viscous mixture was then left to cool back down to room temperature, which afforded the formation of a brownish gel.

Characterization of the GPEs

The morphologies of the synthesized GPEs were investigated by field emission scanning electron microscopy (FESEM) using a FEI Quanta field emission gun 450 at 5 kV. The degree of crystallinity of the samples was investigated by powder XRD performed on a PANalytical Empyrean diffractometer at 2θ values between 5 and 80° at 298 K using a $\text{Cu } K_{\alpha}$ ($\lambda = 1.54056 \text{ \AA}$) radiation source and a step size of 0.0260°. The complexation behaviour of PVA-*co*-PE copolymer in the presence of MPII ionic liquid and NaI were investigated using FTIR using a Thermo Scientific Nicolet ISIO Smart ITR under transmittance mode. The samples were scanned between 4000 and 500 cm^{-1} at a resolution of 1 cm^{-1} . Electrochemical impedance spectroscopy (EIS) was carried out on a HIOKI Model 3532-50 HiTESTER interfaced with a computer to determine the ionic conductivity and dielectric behaviour of the GPEs. Samples were sandwiched between two blocking platinum electrodes (with the thickness of 0.28 cm and cross-sectional area of 2.27 cm^2), and the frequency range used was between 50 and 5 MHz. Temperature-dependent EIS measurements were performed between 30 and 100 °C at 10 °C intervals. Each sample was allowed to reach thermal equilibrium (approximately 30 min) before a measurement was taken. A 400-MHz Bruker Avance III HD SS-NMR spectrometer (Germany) was used to perform the solid state nuclear magnetic resonance (NMR). GPE samples were first cut into thin

Table 1 Compositions of the GPEs with different amount of MPII

Designation	MPII (g)	wt% of MPII
IL0	0.00	0
IL2.5	0.05	2.5
IL5.0	0.10	5.0
IL7.5	0.15	7.5
IL10.0	0.20	10.0
IL12.5	0.25	12.5
IL15.0	0.30	15.0

films (approximately 1.0 mm^2) using a clean razor blade. Sodium spectra were recorded at a frequency of 105.85 MHz using direct excitation with a recycle delay of 1 s and a spin rate of 10 kHz. Sodium spectra were referenced with respect to 1 M NaCl. The magic angle was set to be at 54.71° . The measurements were performed between -20 and 60°C at approximately 10°C intervals. Differential scanning calorimetry analysis of the samples was conducted using DSC Q20. The specific amount of each sample (5–10 mg) was taken in aluminium pan, and the empty aluminium pan was used as a reference. The analysis was carried out from room temperature to 400°C under inert atmosphere of nitrogen gas at the heating rate of $10^\circ\text{C}/\text{min}$.

Fabrication and characterization of DSSCs

Fabrication of working electrode

Absolute ethanol (EtOH) was purchased from Fluka, USA, while P25 titanium dioxide (TiO_2), P90 TiO_2 nanoparticles, and Triton X-100 were purchased from Sigma-Aldrich (Kuala Lumpur, Malaysia). Nitric acid (HNO_3) (65% v/v aqueous solution) were used as received from Friendemann Schmidt Chemical (Kuala Lumpur, Malaysia). Firstly, fluorine-doped tin oxide (FTO) conducting glass substrates (purchased from Solaronix, Switzerland, with sheet resistance of $8 \Omega \text{ sq.}^{-1}$) were cut into smaller pieces of $2 \times 2 \text{ cm}^2$ sheets. FTO conducting glass substrates was cleaned in a sonication bath in deionized water followed by EtOH for 2 min each. The FTO substrates were then spin-coated with of P90 TiO_2 nanoparticles (0.5 g) suspended in HNO_3 (2 mL adjusted to pH 1) to form a compact layer. The substrate was sintered in furnace at 450°C for 30 min before applying a second TiO_2 layer: A paste containing P25 TiO_2 (0.5 g) and five drops of Triton X-100 was prepared in HNO_3 (2 mL adjusted to pH 1) and coated on top of the titanated substrate using the doctor blade method. The substrate was again sintered in furnace at 450°C for 30 min. The substrate was immersed in di-tetrabutylammonium *cis*-bis(isothiocyanato)bis(2,2'-bipyridyl-4,4'-dicarboxylato)rythenium(II), N719 dye solution (5 mL of a 1 mg/mL solution in EtOH) for 24 h. The substrate was finally dried gently using lens cleaning tissue.

Fabrication of counter electrode

The platinum (Pt) paste was synthesized using a solution consisting of the chloroplatinic acid solution (H_2PtCl_6) and ethanol. A few drops of the solution were cast on the conducting surface of the FTO glass and air dried for 30 min. Then, the electrodes were sintered at 450°C for 30 min. The sintered electrodes were gently rinsed with EtOH, and the procedure above were repeated twice.

Fabrication and characterization of DSSCs

The DSSCs were fabricated by sandwiching the prepared GPE between the working and counter electrodes. ABET Technologies solar simulator fitted to a Metrohm Autolab potentiostat (PGSTAT128N) was used to characterize the performance of DSSCs. The photocurrent-voltage (J - V) characteristics were measured under an illumination intensity of 100 mW cm^{-2} . The active area of DSSC was between 0.25 and 0.30 cm^2 , and the data were averaged from measurements on three identical devices. EIS of DSSC was measured in the range of 0.05 to 100 kHz using a DC potential bias with an AC open circuit voltage potential of 10 mV .

Results and discussion

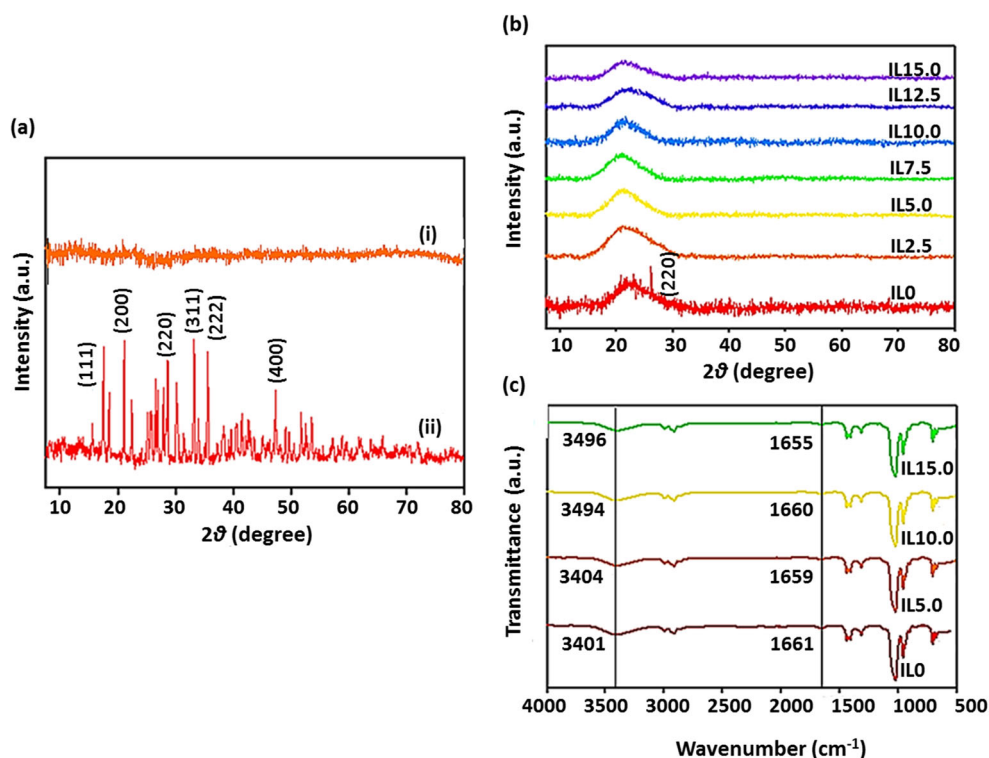
Characterization of GPEs

The XRD diffractogram for the pure compounds (NaI salt and PVA-*co*-PE) were shown in Fig. 1a. The absence of sharp features in pure PVA-*co*-PE indicates their amorphous nature. The addition of NaI increases the crystallinity of the pure PVA-*co*-PE as indicated by the increase of height of the broad peak (maxima at $2\theta = 21.5^\circ$) observed in the spectra of IL0 (Fig. 1b). However, the absence of almost all original peaks of NaI (except for the peak located at 26.2°) in the IL0 sample demonstrates a nearly complete dissociation of salt into the polymer network, in accordance with the literature [10]. In addition, this also illustrates that no new phase is found in the complex. The peak located at 26.2° observed in the spectra of IL0 can be assigned to (220) reflection of NaI [11], which indicates that there is still a small amount of NaI that remains as ion pairs. On the other hand, all MPII-modified GPEs also display single broad diffraction peak with maxima at approximately the same Bragg angle ($2\theta = 21.2^\circ, 21.9^\circ, 21.3^\circ, 21.7^\circ, 22.6^\circ$, and 21.4° for IL2.5, IL5.0, IL7.5, IL10.0, IL12.5, and IL15.0, respectively). It was observed that the height of the single broad peaks of all GPE samples decrease following the addition of MPII ionic liquid. Besides, the degree of reduction of the height has a positive correlation with the amount of MPII added. This indicates that the addition of MPII reduces the overall degree of crystallinity of the samples [12]. By calculating the coherent length of the GPEs sample, we can conclude that the sample have the amorphous structure which it has lower degree crystallinity. The degree of crystallinity among all the samples could be compared by calculating the coherent length by using the Scherrer equation:

$$\tau = K\lambda/(\beta \cos\theta) \quad (1)$$

where τ is the coherent length in nm; K is a dimensionless shape factor (the typical value of 0.9 was used in our case); λ

Fig. 1 **a** XRD pattern of (i) pure P(VA-co-PE) and (ii) pure NaI. **b** XRD pattern of IL0, IL2.5, IL5.0, IL7.5, IL10.0, IL12.5, and IL15.0. **c** FTIR spectra of IL0, IL5.0, IL10.0, and IL15.0



is the wavelength of the X-ray in nm; β is the line broadening at half the maximum intensity in rad; and θ is the Bragg angle in $^\circ$. The values of coherent length as tabulated in Table 2 agree with the XRD data where the lower the degree of crystallinity of the GPEs, the smaller the value of the coherent length. The cations of MPII are bulky, asymmetrical, and not planar in nature, and they make the overall complex much harder to arrange itself into an orderly structure. This property of MPII is of great importance towards the increase of mobility of the charge carriers.

The complexation between the MPII, PVA-co-PE, and NaI which creates more conducting path for the transport of the ions is displayed in Fig. 1c. The shifting of the characteristic peaks was tabulated in Table 3. It was observed that the biggest shifting was the O–H stretching peak. This is due to the fact that O–H bond is the only polar bond found in the PVA-co-PE copolymer. It interacts more strongly with MPII ionic liquid and causes a larger shifting compared with other non-polar bonds

Table 2 Coherent length of GPE samples with different concentrations of MPII

Electrolytes	Coherent length, τ (nm)
IL0	1.54
IL2.5	1.53
IL5.0	1.47
IL7.5	1.41
IL10.0	1.37
IL12.5	1.37
IL15.0	1.30

such as C–H bond and C–C bond. The peak that originally located at 3401 cm^{-1} was shifted to 3404 cm^{-1} , 3394 cm^{-1} , and 3396 cm^{-1} in IL5.0, IL 10.0, and IL15.0, respectively. On the other hand, the reason behind the plummeting of ionic conductivity after the optimal value (e.g. IL 12.5 and IL15.0) can be attributed to the formation of ion pair clusters. At higher concentration of ionic liquid, the ions fail to dissociate and remain in the form of ion pair. The ion pairs not only do not contribute to the overall ionic conductivity—since they behave like a compound as a whole rather than free individual ion—but they also hinder the mobility of other free ions and block their transportation within the polymer electrolyte [13].

The Cole-Cole plots of the GPE samples are shown in Fig. 2a. The bulk resistance, R_b , is measured from the Cole-Cole plot by extrapolating the semicircle region to its highest frequency while the ionic conductivity (σ) is computed using the following formula:

$$\sigma = t/R_b A \quad (2)$$

where t is the thickness of the GPE samples; R_b is the bulk resistance; and A is the cross-sectional area. Notably, only a

Table 3 Shifting of the characteristic peaks with the addition of MPII

Band assignments	Wavenumber (cm^{-1})			
	IL0	IL5.0	IL10.0	IL15.0
Stretching of O–H bond	3401	3404	3494	3496
Bending of C–H bond	1661	1659	1660	1655

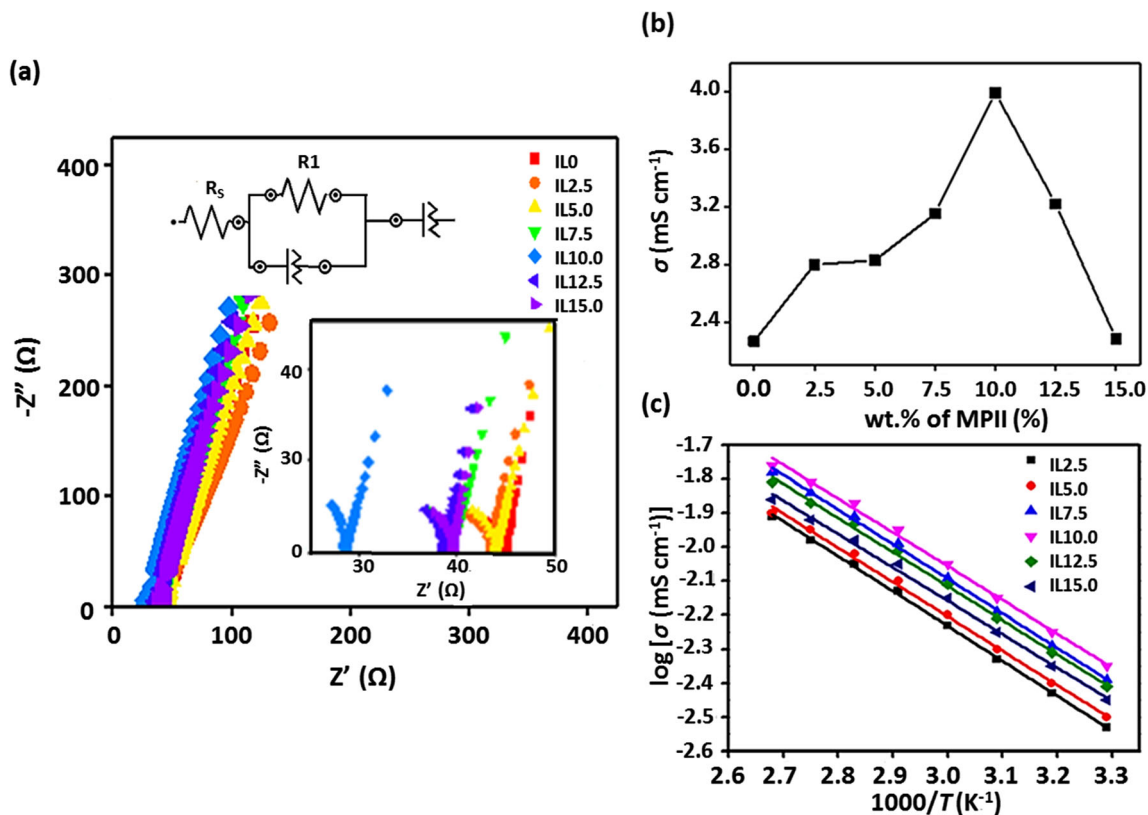


Fig. 2 a The Cole-Cole plot of the GPE samples indicating the changes in the R_p with the variation of the amount of MPII ionic liquid. **b** Ionic conductivity of the GPE samples as a function of amount of MPII ionic

liquid. **c** The Arrhenius plot obtained from the temperature dependence ionic conductivity studies indicating that the samples exhibit typical Arrhenius behaviour

small part of the semi-circular region of the Cole-Cole plot can be observed. This signifies that the conductivity is contributed dominantly by free ions rather than electron. Figure 2b shows the ionic conductivity of the GPE samples. The maximum ionic conductivity of 3.99 mS cm⁻¹ is observed in IL10.0. The ionic conductivity of the GPE samples (e.g. IL2.5, IL5.0, and IL 7.5) increases proportionately with the concentration of MPII ionic liquid increases up until an optimal point in IL10.0 before falling. This phenomenon is explained using the equation for ionic conductivity:

$$\sigma(T) = \sum_i n_i q_i \mu_i \tag{3}$$

where n represents the density of charge carriers; q indicates the charge of ions; and μ represents the mobility of the ions. Since the type of ions is fixed in this experiment (both salt and ionic liquid), the difference in the ionic conductivity comes entirely from the variation of the charge carrier density and its mobility. When a small amount of MPII ionic liquid is added, it dissociates and increases the charge carrier density. As a result, it increases the overall ionic conductivity [14]. Besides, from the results of XRD diffractogram, it was also observed that the addition of MPII ionic liquid decreases the degree of crystallinity of the GPE samples which indicates that the existence of MPII creates more amorphous region within the GPE which is beneficial for the ion diffusion [15,

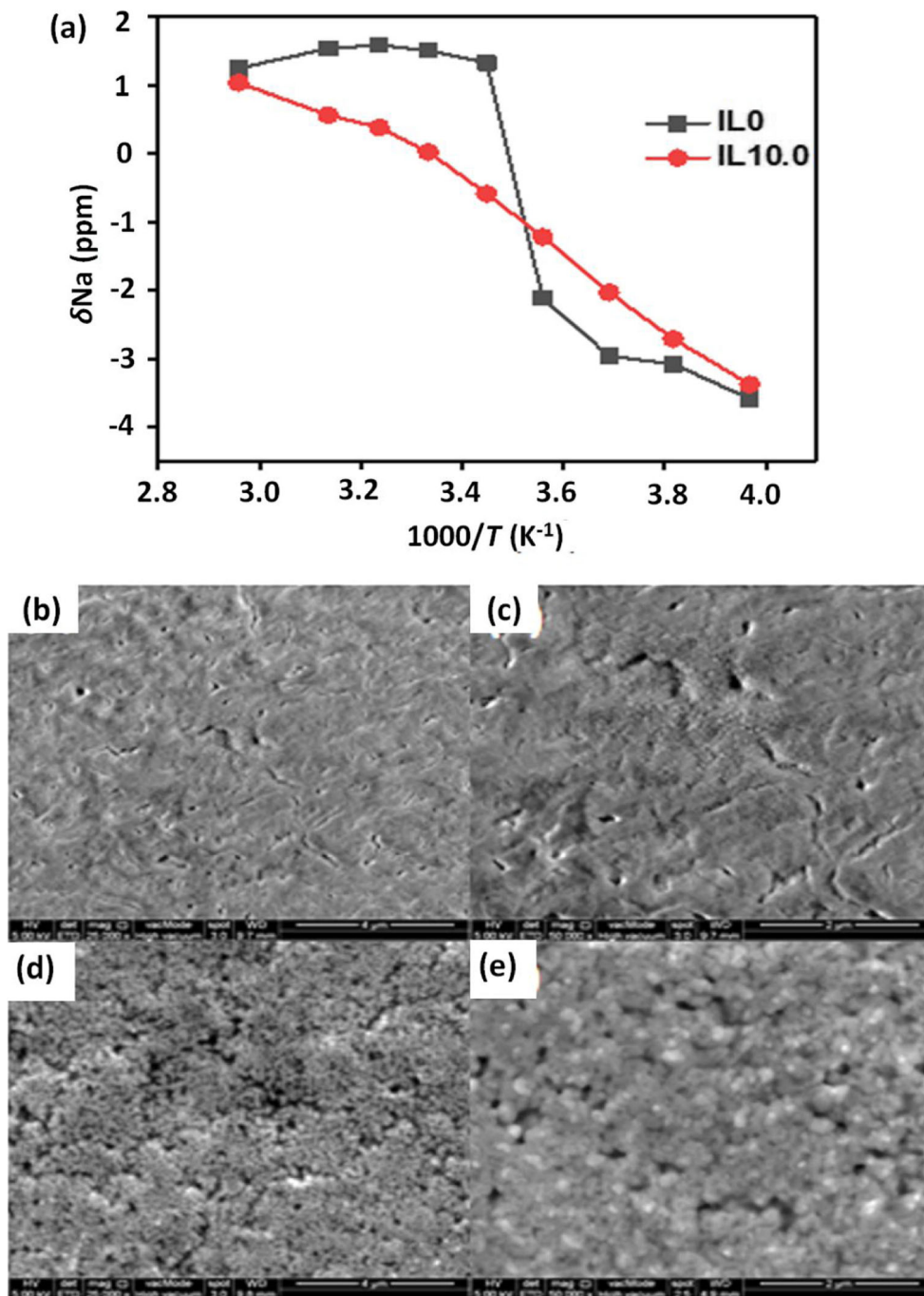
liquid. **c** The Arrhenius plot obtained from the temperature dependence ionic conductivity studies indicating that the samples exhibit typical Arrhenius behaviour

16]. This also indicates that MPII acts as a plasticizer that helps to increase the segmental flexibility of the PVA-co-PE backbone. When it comes to the temperature dependence studies, the Arrhenius plot of the GPE samples was plotted in Fig. 2c, and activation energies of the GPE samples were summarized in Table 4. From the plots, it is clear that every sample exhibits linear behaviour, as indicated by an R^2 value of > 0.96 for each sample, which corresponds to Arrhenius behaviour. Hence, it can be concluded that the ion transport mechanism is governed by ion hopping mechanism. The free ions (the O–H bond of PVA-co-PE copolymer) will dominantly be hopping between the coordinating sites. At higher temperature, charge carriers gain more thermal energy, and both

Table 4 The activation energy of the GPE samples with the variation of amount of MPII ionic liquid

Gel polymer electrolyte	Activation energy, E_a (eV)	R squared value
IL2.5	0.194 ± 0.005	0.996
IL5.0	0.18 ± 0.01	0.963
IL7.5	0.176 ± 0.003	0.998
IL10.0	0.139 ± 0.006	0.987
IL12.5	0.190 ± 0.005	0.996
IL15.0	0.20 ± 0.01	0.976

Fig. 3 **a** Temperature-dependent ^{23}Na NMR resonance shift of both IL0 and IL 10.0 samples. FESEM image of **b** IL0 at 25,000 \times , **c** IL0 at 50,000 \times , **d** IL10.0 at 25,000 \times , and **e** IL10.0 at 50,000 \times



the intermolecular hopping and intramolecular hopping become more frequent. As a result, the ionic conductivity increases [17, 18]. The activation energy of the GPE samples was determined following the Arrhenius equation:

$$\sigma(T) = \sigma_o \exp(E_a/RT) \quad (4)$$

where σ is the ionic conductivity; σ_o is the pre-exponential constant; T is temperature (in Kelvin); R is the universal gas constant; and E_a is the activation energy. Equation 3 states that the trend of activation energy is inversely proportional

to ionic conductivity (in which IL10.0 has the lowest activation energy but highest ionic conductivity).

The ^{23}Na NMR resonance of both IL0 and IL10.0 at different temperatures was performed to study the interaction of the sodium ions with its surrounding atoms. The results were summarized in Fig. 3a. It was noticed that the shifted ^{23}Na NMR resonance increases with increasing temperature which means that the peak found in the ^{23}Na NMR resonance was shifted downfield. For IL10.0, the variation of the shifted ^{23}Na NMR resonance is qualitatively similar to those found in the

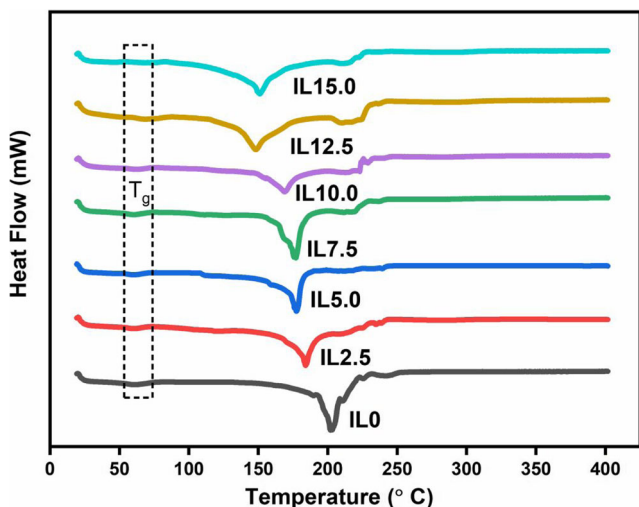


Fig. 4 DSC curves of the samples

room-temperature ionic conductivity studies. However, in the case of IL0, the sudden plummeting in the shifted ²³Na NMR resonance at 290 K implied that there is a phase transition occurring at that temperature. It was suspected to be the glass transition (*T_g* for pure PVA-co-PE is at 320 K) [19] since the melting peak of PVA-co-PE copolymer was located at a much higher temperature (at approximately 430 K). IL10.0 does not experience the same drastic shift of ²³Na NMR resonance at the temperatures tested within the range of temperature in which the experiment was carried out. This implied that the glass transition temperature of the electrolyte is lowered by the addition of MPII ionic liquid [20]. Figure 3b–e show the FESEM images of IL0 and IL10.0. Although low degree of porosity (diameter size approximately 0.2 μm) was observed in IL0, the overall morphology was considered to be relatively smooth. The opposite is true after the addition of MPII ionic liquid, where no visible pores were noticed, but the roughness is much higher.

DSC analysis was conducted to observe the glass transition temperature of PVA-co-PE and MPII-modified GPE. Figure 4 shows the DSC thermograms of PVA-co-PE and MPII-modified GPE. The glass transition temperature (*T_g*) for IL0, IL2.5, IL5.0, IL7.5, IL10, IL12.5, and IL15 are given in Table 5. It can be seen from the DSC thermograms and glass

Table 5 Glass transition temperature of GPEs

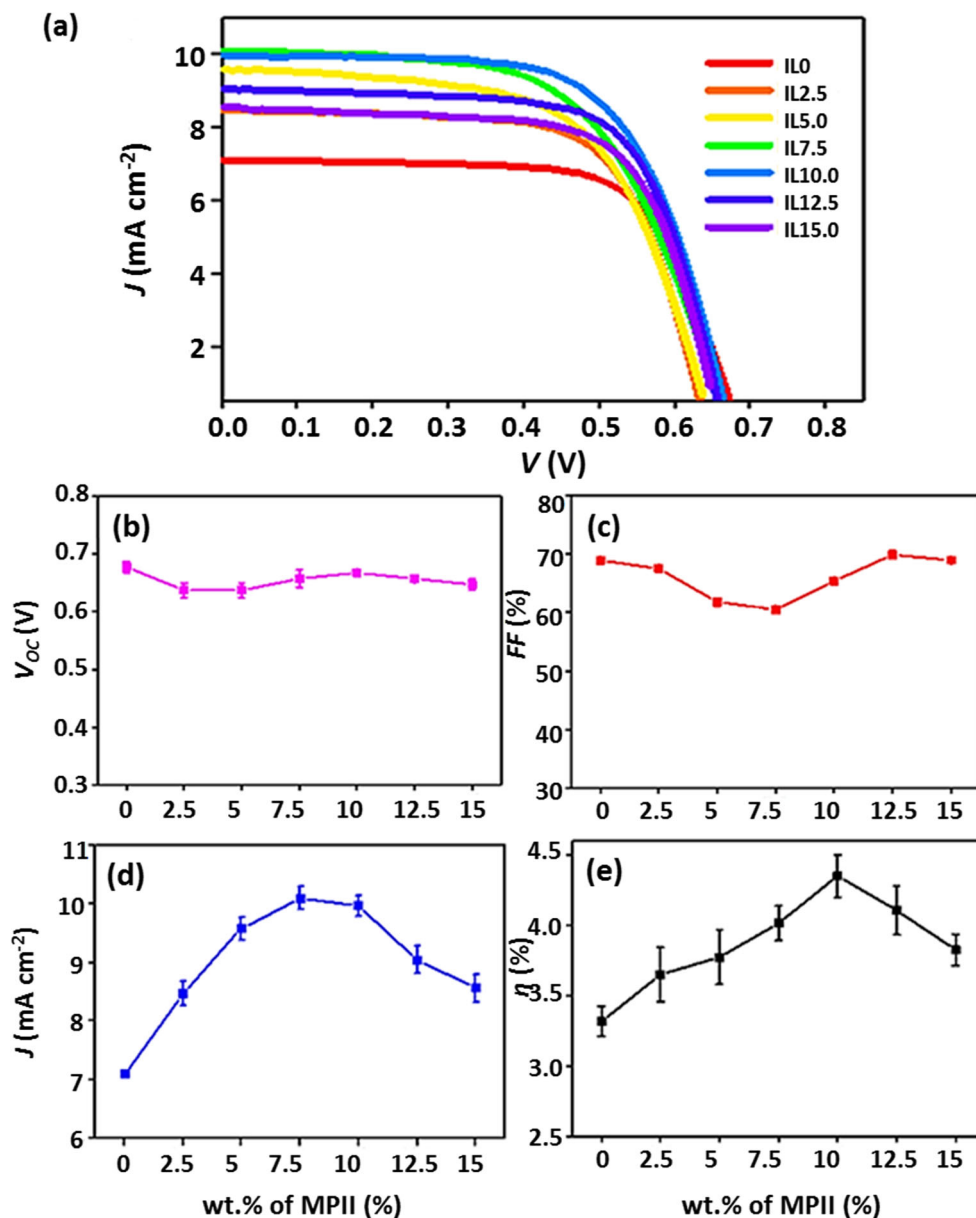
Electrolytes	Glass transition temperature (°C)
IL0	59.0
IL2.5	60.0
IL5	60.4
IL7.5	61.1
IL10	63.1
IL12.5	67.5
IL15	68.9

transition temperature that there is a slight increase in *T_g* after addition of MPII ionic liquid. The glass transition temperature of PVA-co-PE is 59.0 °C which is in good agreement with the reported literature [21]. The thermal results reveal the slight increase in *T_g* which is due to the complexation between copolymer and ionic liquid. Since the increase in ionic conductivity with addition of MPII may be due to increasing number of charge carriers, therefore the *T_g* became slightly changed with different MPII weight ratios [22]. Consequently, it can be stated that the introduction of amorphous ionic liquid improves the ionic conductivity of the gel polymer electrolyte by reducing the polymer electrolyte crystallinity [23].

Characterization of DSSCs

Figure 5a shows the *J–V* curve of the assembled DSSCs. The DSSC parameters such as open-circuit voltage (*V_{OC}*), fill factor (*FF*), short-circuit current density (*J_{SC}*), and efficiency (*η*) were calculated and plotted in Fig. 5b–e, respectively. The *V_{OC}* values in Fig. 5b remains constant in the range of 0.637–0.667 V. *V_{OC}* depends on Fermi level of the TiO₂ nanoparticles as well as the potential of the redox mediator which are all fixed in this experiment. Thus, only a small fluctuation of *V_{OC}* is observed. From Fig. 5c, it was observed that *FF* exhibits a relatively similar trend with *V_{OC}* in the range of 60.5–69.9%. The short circuit current density *J_{SC}* in Fig. 5d increases with the amount of MPII ionic liquid and reaches the maximum of 10.09 mA cm⁻² at IL7.5. Although IL10.0 does not have the highest *J_{SC}*, its value is just slightly lower than that of IL7.5 (~1%) and this falls within the uncertainty of the experiment. Last but not least, the photon conversion efficiency of the DSSC increases when more MPII ionic liquid is added as shown Fig. 5e. The GPE containing 10 wt% of MPII ionic liquid has achieved the highest photon conversion efficiency of 4.35%. This has proven that even a small amount of MPII ionic liquid can improve (31% improvement) the performance of DSSCs given that IL0 only has an efficiency of 3.32%. The presence of MPII increases the number of iodide/triiodide (Γ/Γ^{-3}) ions within the GPE. This is favourable in DSSC as Γ/Γ^{-3} ions are the main contributor in completing the DSSCs circuit by releasing and accepting the electrons from both electrodes. Not only that MPII enhances the homogeneity of the GPE, it also decreases the overall crystallinity and improves the surface contact with the electrodes. The trend of efficiency was also in good agreement with the results obtained from the ionic conductivity studies. Table 6 shows the comparison for the efficiency of some DSSCs in recent literature. Based on this work, it has been shown that significant improvements have been achieved in improving the GPEs based on MPII ionic liquid as additive. Among DSSCs

Fig. 5 **a** J–V curve of the DSSCs fabricated using GPE samples with different amount of MPII ionic liquid. The variation of the DSSC parameters, **b** fill factor, **c** open-circuit voltage, **d** short-circuit current density, and **e** efficiency with different amount of MPII ionic liquid



employing MPII, Khanmirzaei et al. presented an efficiency of 2.09% using rice starch as the host polymer, NaI dopant salt, and 20 wt% of MPII ionic liquid [24]. Nadia

et al. achieved an efficiency of 2.16% with 3.0 g of MPII ionic liquid and agar natural polymer [25]. Thus, it can be concluded that PVA-co-PE copolymer is a better candidate as the host polymer in terms of the efficiency obtained as compared with other polymers stated above. This might be due to the reason that PVA-co-PE consists of more polar groups than rice starch and agar natural polymer. Conversely, raising the addition of MPII ionic liquid to 12.5 and 15 wt% has dropped the efficiency of DSSC, which is indicative to the effect of excess ion accumulation. These phenomena causes the free ions to form neutral pairs which resulted in the reduction of ionic mobility in the GPE. The efficiency value is strongly dependent on the mobility of Γ^- / Γ^3 ions. On the whole, these data reveal that the introduction of 10 wt% MPII

Table 6 The comparison of efficiency with other DSSC results

Electrolytes system	Efficiency, η (%)	References
HPC-NaI-MPII	5.79	[22]
Agar-KI-MPII	2.16	[25]
Rice starch-NaI-MPII	2.09	[24]
P(EO-PO)-LiI-MPII	3.66	[26]
PVdf-HFP-MPII	3.70	[27]

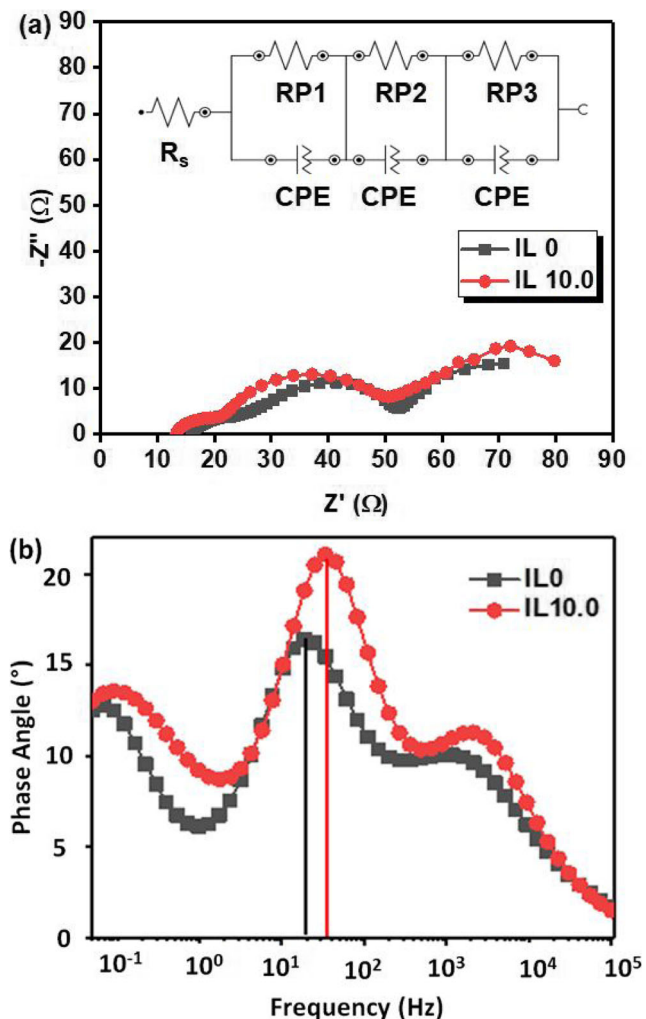


Fig. 6 a EIS spectra of DSSC assembled using IL0 and IL10.0. b The Bode phase plot of IL0 and IL10.0

ionic liquid into the GPE is the optimum MPII concentration.

Figure 6a shows the EIS spectra of DSSCs fabricated using electrolyte with and without ionic liquid, IL0 and IL10.0. The data obtained from the experiment was fitted using the Metrohm Autolab Nova 2.1.2 software. The inset shows the equivalent circuit, and the fitted data was summarized in Table 7. Three semicircles were found in the fitted data. In the order of increasing Z' (or decreasing frequency), the first semicircle represents the regeneration of Γ^- ions at the counter electrode/electrolyte interface as well as the uncovered FTO/electrolyte interface, and the parameter used to fit this semicircle was RP1. The

Table 7 The fitted parameter of the EIS spectra for IL0 and IL10.0

Electrolyte	R_s (Ω)	RP1 (Ω)	RP2 (Ω)	RP3 (Ω)	τ (ms)
IL0	15.7 ± 0.1	11.7 ± 0.9	25 ± 1	41 ± 5	54 ± 1
IL10.0	13.2 ± 0.1	8.3 ± 0.6	27 ± 2	70 ± 10	22.0 ± 0.7

second and third semicircle give information regarding the electron diffusion in the TiO_2 nanoparticles and the resistance of the electrons recombination process with redox mediator as well as the diffusion rate of redox mediator in the electrolyte, respectively [24, 28]. The parameters employed to fit them are RP2 and RP3. The last parameter used in fitting the EIS spectra is R_s which represents the overall series resistance of the counter electrode/electrolyte interface, electrolyte, and working electrode/electrolyte interface [28].

The observed values of RP2 using two different GPEs were quite similar so Bode phase plot was plotted in Fig. 6b. It was observed that both curves have a distinct peak in the frequency range of 10 to 100 Hz. These peaks correspond to the injected electron recombination resistance [29], and the electron lifetime was calculated using the following equation:

$$\tau = 1/f_p \tag{5}$$

where τ is the electron lifetime, and f_p is the recombination frequency. The peak has been shifted to the higher frequency after the addition of MPII into the GPE which indicates a higher electron recombination resistance. This observation is supported by the similar works conducted by Sundararajan and Mohamad Sri where the resistance of the electron recombination process was increased with increasing the concentration of ionic liquid [30, 31]. High electron recombination resistance reduces the tendency of electrons to recombine with Γ/Γ^- ions in GPEs. This prevents the back reaction of electrons within the TiO_2 conduction band, thus, extending the effective electron lifetime and overall performance of the present DSSC devices.

Conclusion

DSSCs with higher efficiency was successfully fabricated using MPII/PVA-co-PE/ I_2 /DMSO/NaI GPE. The incorporation of MPII has increases the ionic conductivity of the GPE, and the maximum ionic conductivity obtained is 3.99 mS cm^{-1} at 10 wt% of MPII. All samples were found to follow Arrhenius behaviour in the temperature range of 303 to 373 K. The results obtained from structural studies reveal that the addition of MPII ionic liquid reduces the overall degree of crystallinity of the GPE samples. Complexation studies confirm the existence of interaction between the NaI salt, PVA-co-PE copolymer, and the MPII ionic liquid. The DSSC with the highest photon conversion efficiency of 4.35%, along with J_{SC} of 9.97 mA cm^{-2} , V_{OC} of 0.67 V, and fill factor of 65.39% was obtained using 10 wt% of MPII.

Funding information This research is funded by University of Malaya Research Grant (RG382-17AFR) and Fundamental Research Grant Scheme (FRGS) from the Ministry of Education, Malaysia (FP062-2018A). S.R. gratefully acknowledges the Institute of Advance Studies

at Durham University for the award of a Durham International Fellowship for Research and Enterprise (DIFeREns2) Senior Research Fellowship, a project of the European Union's Seventh Framework Programme, to carry out part of this collaborative work in the United Kingdom. M.M.A. acknowledges the King Khalid Military Academy for funding his sabbatical at Durham University to engage in this work.

References

- O'Regan B, Gratzel M (1991) A low-cost, high-efficiency solar-cell based on dye-sensitized colloidal TiO₂ films. *Nature* 353:737–740. <https://doi.org/10.1038/353737a0>
- Campbell WM, Burrell AK, Officer DL, Jolley KW (2004) Porphyrins as light harvesters in the dye-sensitized TiO₂ solar cell. *Coord Chem Rev* 248:1363–1379. <https://doi.org/10.1016/j.ccr.2004.01.007>
- Kakiage K, Aoyama Y, Yano T, Oya K, Fujisawa J, Hanaya M (2015) Highly-efficient dye-sensitized solar cells with collaborative sensitization by silyl-anchor and carboxy-anchor dyes. *Chem Commun* 51:15894–15897. <https://doi.org/10.1039/C5CC06759F>
- Stergiopoulos T, Rozi E, Karagianni CS, Falaras P (2011) Influence of electrolyte co-additives on the performance of dye-sensitized solar cells. *Nanoscale Res Lett* 6:6–7. <https://doi.org/10.1186/1556-276X-6-307>
- Sakaguchi S, Ueki H, Kato T et al (2004) Quasi-solid dye sensitized solar cells solidified with chemically cross-linked gelators. Control of TiO₂/gel electrolytes and counter Pt/gel electrolytes interfaces. *J Photochem Photobiol A Chem* 164:117–122. <https://doi.org/10.1016/j.jphotochem.2003.11.014>
- Chen PY, Lee CP, Vittal R, Ho KC (2010) Iodine-free high efficient quasi solid-state dye-sensitized solar cell containing ionic liquid and polyaniline-loaded carbon black. *J Power Sources* 195:3933–3938. <https://doi.org/10.1016/j.jpowsour.2009.12.086>
- Sugumaran T, Silvaraj DS, Saidi NM, Farhana NK, Ramesh S, Ramesh K, Ramesh S (2019) The conductivity and dielectric studies of polymer electrolytes based on iota-carrageenan with sodium iodide and 1-butyl-3-methylimidazolium iodide for the dye-sensitized solar cells. *Ionics (Kiel)* 25:763–771. <https://doi.org/10.1007/s11581-018-2756-3>
- Syairah A, Khanmirzaei MH, Saidi NM, Farhana NK, Ramesh S, Ramesh K, Ramesh S (2018) Effect of different imidazolium-based ionic liquids on gel polymer electrolytes for dye-sensitized solar cells. *Ionics (Kiel)* 25:2427–2435. <https://doi.org/10.1007/s11581-018-2603-6>
- Tan CY, Farhana NK, Saidi NM et al (2018) Conductivity, dielectric studies and structural properties of P(VA-co-PE) and its application in dye sensitized solar cell. *Org Electron* 56:116–124. <https://doi.org/10.1016/j.orgel.2018.02.007>
- Tretinnikov ON, Zagorskaya SA (2012) Determination of the degree of crystallinity of poly(vinyl alcohol) by ftir spectroscopy. *J Appl Spectrosc* 79:521–526. <https://doi.org/10.1007/s10812-012-9634-y>
- Adham M, Rezagholipour Dizaji H, Fazli M (2019) Growth and investigation of pure and sodium iodide-doped zinc tris-thiourea sulphate (ZTS) single crystals. *Mater Res Innov* 23:222–227. <https://doi.org/10.1080/14328917.2018.1435383>
- Karthika P, Ganesan S, Arthanareeswari M (2018) Low-cost synthesized organic compounds in solvent free quasi-solid state polyethyleneimine, polyethylene glycol based polymer electrolyte for dye-sensitized solar cells with high photovoltaic conversion efficiencies. *Sol Energy* 160:225–250. <https://doi.org/10.1016/j.solener.2017.11.076>
- Androsch R, Monami A, Kucera J (2014) Effect of an alpha-phase nucleating agent on the crystallization kinetics of a propylene/ethylene random copolymer at largely different supercooling. *J Cryst Growth* 408:91–96. <https://doi.org/10.1016/j.jcrysgro.2014.09.028>
- Watanabe M, Ogata N (1988) Ionic conductivity of polymer electrolytes and future applications. *Br Polym J* 20:181–192. <https://doi.org/10.1002/pi.4980200304>
- Pang HW, Yu HF, Huang YJ et al (2018) Electrospun membranes of imidazole-grafted PVDF-HFP polymeric ionic liquids for highly efficient quasi-solid-state dye-sensitized solar cells. *J Mater Chem A* 6:14215–14223. <https://doi.org/10.1039/c8ta01215f>
- Chaurasia SK, Saroj AL, Shalu et al (2015) Studies on structural, thermal and AC conductivity scaling of PEO-LiPF₆ polymer electrolyte with added ionic liquid [BMIMPF₆]. *AIP Adv* 5:077178. <https://doi.org/10.1063/1.4927768>
- Nei de Freitas J, Nogueira AF, De Paoli M-A (2009) New insights into dye-sensitized solar cells with polymer electrolytes. *J Mater Chem* 19:5279. <https://doi.org/10.1039/b900928k>
- Saidi NM, Ng HM, Omar FS et al (2019) Polyacrylonitrile-poly(1-vinyl pyrrolidone-co-vinyl acetate) blend based gel polymer electrolytes incorporated with sodium iodide salt for dye-sensitized solar cell applications. *J Appl Polym Sci* 136:47810. <https://doi.org/10.1002/app.47810>
- Hashmi SG, Ozkan M, Halme J et al (2015) High performance dye-sensitized solar cells with inkjet printed ionic liquid electrolyte. *Nano Energy* 17:206–215. <https://doi.org/10.1016/j.nanoen.2015.08.019>
- Kawano R, Matsui H, Matsuyama C et al (2004) High performance dye-sensitized solar cells using ionic liquids as their electrolytes. *J Photochem Photobiol A Chem* 164:87–92. <https://doi.org/10.1016/j.jphotochem.2003.12.019>
- Seethamraju S, Ramamurthy PC, Madras G (2013) Flexible poly(vinyl alcohol-co-ethylene)/modified MMT moisture barrier composite for encapsulating organic devices. *RSC Adv* 3:12831–12838. <https://doi.org/10.1039/c3ra41557k>
- Khanmirzaei MH, Ramesh S, Ramesh K (2015) Hydroxypropyl cellulose based non-volatile gel polymer electrolytes for dye-sensitized solar cell applications using 1-methyl-3-propylimidazolium iodide ionic liquid. *Sci Rep* 5:1–7. <https://doi.org/10.1038/srep18056>
- Aram E, Ehsani M, Khonakdar HA (2015) Improvement of ionic conductivity and performance of quasi-solid-state dye sensitized solar cell using PEO/PMMA gel electrolyte. *Thermochim Acta* 615:61–67. <https://doi.org/10.1016/j.tca.2015.07.006>
- Khanmirzaei MH, Ramesh S, Ramesh K (2015) Polymer electrolyte based dye-sensitized solar cell with rice starch and 1-methyl-3-propylimidazolium iodide ionic liquid. *Mater Des* 85:833–837. <https://doi.org/10.1016/j.matdes.2015.06.113>
- Nadia SR, Khanmirzaei MH, Ramesh S, Ramesh K (2017) Quasi-solid-state agar-based polymer electrolytes for dye-sensitized solar cell applications using imidazolium-based ionic liquid. *Ionics (Kiel)* 23:1585–1590. <https://doi.org/10.1007/s11581-016-1946-0>
- Freitas FS, Freitas JND, Ito BI et al (2009) Electrochemical and structural characterization of polymer gel electrolytes based on a PEO copolymer and an imidazolium-based ionic liquid for dye-sensitized solar cells. *ACS Appl Mater Interfaces* 1:2870–2877. <https://doi.org/10.1021/am900596x>
- Saaid FI, Tseng TY, Winie T (2019) Effect of ionic liquid concentration on the photovoltaic performance of dye-sensitized solar cell. *Mater Today Proc* 17:401–407. <https://doi.org/10.1016/j.matpr.2019.06.267>
- Hu P, Duan Y, Hu D, Qin B, Zhang J, Wang Q, Liu Z, Cui G, Chen L (2015) Rigid-flexible coupling high ionic conductivity polymer electrolyte for an enhanced performance of LiMn₂O₄/graphite battery at elevated temperature. *ACS Appl Mater Interfaces* 7:4720–4727. <https://doi.org/10.1021/am5083683>

29. Mohd Noor SA, Yoon H, Forsyth M, Macfarlane DR (2015) Gelled ionic liquid sodium ion conductors for sodium batteries. *Electrochim Acta* 169:376–381. <https://doi.org/10.1016/j.electacta.2015.03.024>
30. Sundararajan V, Selvaraj G, Ng HM et al (2017) Exploring the effect of novel N-butyl-6-methylquinolinium bis(trifluoromethylsulfonyl)imide ionic liquid addition to poly(methyl methacrylate-co-methacrylic) acid electrolyte system as employed in gel-state dye sensitized solar cells. *Electrochim Acta* 240:361–370. <https://doi.org/10.1016/J.ELECTACTA.2017.04.097>
31. Mohamad Sri MNS (2017) Effect of 1-butyl-3-methylimidazolium iodide on the performance of dye-sensitized solar cell having PEO-PVA based gel polymer electrolyte. *Mater Today Proc* 4:5161–5168. <https://doi.org/10.1016/J.MATPR.2017.05.022>

Publisher's note Springer Nature remains neutral with regard to jurisdictional claims in published maps and institutional affiliations.